JASA ARTICLE

Interaction effects in laryngeal and respiratory control of the voice source and vocal fold contact pressure

Zhaoyan Zhang[a)]
Department of Head and Neck Surgery, University of California Los Angeles, Los Angeles, California 90095-1794, USA

ABSTRACT:
Previous studies of laryngeal and respiratory control of the voice source often focus on main effects of individual control parameters but not their interactions. The goal of this study is to systematically identify important interaction effects in laryngeal and respiratory control of the voice source and vocal fold contact pressure in a three-dimensional voice production model. Computational simulations were performed with parametric variations in vocal fold geometry, stiffness, prephonatory glottal gap, and subglottal pressure. The results showed that, while the glottal closure pattern and source spectral shape were dominantly controlled by vocal fold vertical thickness, the prephonatory glottal gap had important effects in thick vocal folds or near phonation onset. Coordinated adjustments in both the prephonatory glottal gap and thickness were required to produce a long duration of the closed phase and strong high-frequency harmonic production. Interaction between subglottal pressure and transverse stiffness was observed in the control of the peak vocal fold contact pressure. The contact pressure was highest in vocal folds with low transverse stiffness when exposed to high subglottal pressure, indicating the importance of maintaining a balance between subglottal pressure and transverse stiffness to minimizing vocal fold injury. *© 2024 Acoustical Society of America.*
https://doi.org/10.1121/10.0034708

(Received 15 October 2024; revised 24 November 2024; accepted 3 December 2024; published online 31 December 2024)
[Editor: James F. Lynch] Pages: 4326–4335

I. INTRODUCTION

Human vocal control is achieved through coordinated adjustments in the respiratory, laryngeal, and articulatory systems. The respiratory system controls subglottal pressure and acts as the power source of voice production, whereas laryngeal adjustments posture the vocal folds into desired geometry, stiffness, and position and determine the voice source characteristics. The cause–effect relationship between laryngeal and respiratory control parameters (vocal fold geometry, stiffness, glottal gap, and subglottal pressure) and the produced voice outcomes was investigated in a series of large-scale computational studies (Zhang, 2016, 2019, 2020, 2021, 2023a). With the large number of parametric simulations, these studies were able to isolate the effect of individual laryngeal controls and subglottal pressure on vocal fold vibration, glottal aerodynamics, and acoustics of the voice source and the radiated voice.

A limitation of these previous studies is their focus on the main effects of individual laryngeal control parameters and subglottal pressure, while excluding interaction effects between these control parameters. This exclusion is largely due to the complexity introduced by the large number of independent and dependent variables involved. This is a common challenge in research studies on laryngeal and respiratory control of the voice source, where systematic investigations of the interaction effects are difficult because of the complex physics involved in voice production and the large number of control parameters. As a result, research studies on laryngeal and respiratory vocal control are often limited to main effects or a qualitative description of the interaction effects (e.g., Titze and Talkin, 1979; Scherer *et al.*, 2001; Pickup and Thomson, 2011; Li *et al.*, 2018, 2020; Wang *et al.*, 2021; Alzamendi *et al.*, 2022; Luizard *et al.*, 2023; Madill and Nguyen, 2023; McCollum *et al.*, 2023; Döllinger *et al.*, 2023; Tur *et al.*, 2023).

The goal of this study was to provide a more complete picture of laryngeal and respiratory control of the voice source, by systematically exploring interaction effects between different laryngeal and respiratory control parameters in a three-dimensional voice production model. This study focused on the interaction effects in the control of the glottal closure pattern and spectral shape of the voice source, two important factors determining the produced voice quality, and vocal fold contact pressure, a measure of potential risk of vocal fold injury. While current research and clinical intervention often focus on the prephonatory glottal gap (i.e., vocal fold approximation in the horizontal plane) as viewed from a superior view, our previous studies (Zhang, 2016, 2021, 2023b) showed that the prephonatory glottal gap had only a small main effect on the glottal closure pattern and source spectral shape. Thus, an important research question of this study was whether the prephonatory glottal gap is involved in some interaction effects and thus has more significant local effects than the main effects observed in our previous studies.

a)Email: zyzhang@ucla.edu

JASA
https://doi.org/10.1121/10.0034708

II. METHODS

This study used the same set of simulation data as our previous study (Zhang, 2021). The data were generated in voice simulations using a previously validated three-dimensional, body-cover, continuum model of voice production (Zhang, 2016, 2017). More details of the model can be found in these previous studies. A sketch of the three-dimensional vocal fold model with its geometric control parameters is shown in Fig. 1. The geometric control parameters include vocal fold length L in the anterior-posterior direction, medial-lateral depths of the body and cover layers (D_b and D_c), medial surface vertical thickness T, and initial glottal angle α in the horizontal plane. In humans, vocal fold adduction not only brings the vocal folds closer together, but also increases their medial surface vertical thickness (Zhang, 2023b). Thus, including both the initial glottal gap and vertical thickness as model controls in this study is essential to simulating vocal fold adduction of varying degrees in both the horizontal plane and the vertical dimension.

Mechanically, the control parameters include vocal fold transverse stiffness E_t in the coronal plane and anterior-posterior (AP) shear moduli in the body and cover layers (G_{apb} and G_{apc}). Additional model controls also include the subglottal pressure P_s and vocal tract shape. For this study, to focus on laryngeal control strategies, no vocal tract was included in the voice simulations. Previous studies showed that source-filter interaction in general has only small effects on the voice source, except for conditions with considerable constriction in the vocal tract or when a harmonic approaches a vocal tract resonance (Titze, 2008; Sundberg, 2017; Zhang, 2023a). Table I summarizes the parametric conditions simulated in this study. These ranges of variations for each model control parameters were based on values in the literature (Hollien, 1960; Hollien and Curtis, 1960; Titze and Talkin, 1979; Hirano and Kakita, 1985; Holmberg *et al.*, 1988; Alipour-Haghighi and Titze, 1991; Wu and Zhang, 2016; Zhang *et al.*, 2017), as detailed in Zhang (2021).

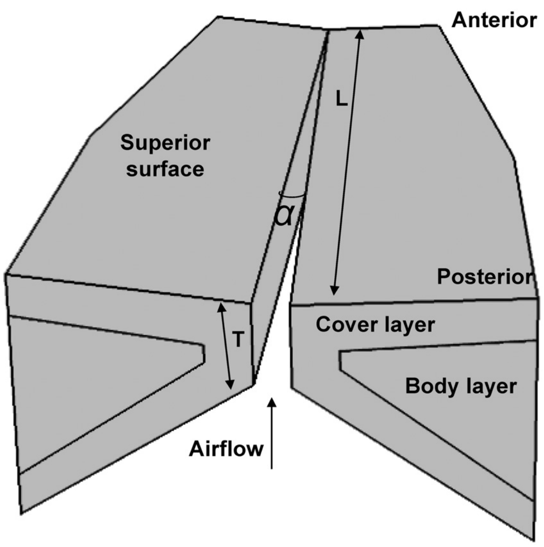

FIG. 1. Sketch of the vocal fold model and its geometric control parameters, including the initial glottal angle α in the horizontal plane, medial surface vertical thickness T, and vocal fold length L. The two medial surfaces form a uniform glottal channel in the coronal plane.

TABLE I. Ranges of model control parameters. For all conditions, the vocal fold density was 1030 kg/m^3, and the AP Poisson's ratio was 0.495. See Zhang (2021) for details.

Transverse Young's modulus	$E_t = [1, 2, 4]$ kPa
Cover AP shear modulus	$G_{apc} = [1, 10, 20, 30, 40]$ kPa
Body AP shear modulus	$G_{apb} = [1, 10, 20, 30, 40]$ kPa
Vertical thickness	$T = [1, 2, 3, 4.5]$ mm
Cover layer depth	$D_c = [1, 1.5]$ mm
Body layer depth	$D_c = [4, 6, 8]$ mm
Vocal fold length	$L = [6, 10, 17]$ mm
Initial glottal angle	$\alpha = [0°, 1.6°, 4°, 8°]$
Subglottal pressure	$P_s = 50$ Pa, 100–1000 Pa in steps of 100 Pa, 1200–2400 Pa in steps of 200 Pa

For each simulation condition, a half second-long sustained phonation was simulated. Measures of vocal fold vibration, glottal flow, and source acoustics were extracted from the produced voice. The measures of vocal fold vibration include the mean (Ag0) and peak-to-peak amplitude (Agtamp) of the glottal area waveform. The glottal flow measures include the mean (Qmean) and peak-to-peak amplitude (Qamp) of the glottal flow waveform, and the maximum flow declination rate (MFDR). The normalized MFDRn was further calculated by normalizing the MFDR by the product of Qamp and the fundamental frequency (F0). Note that the MFDRn is the inverse of the normalized amplitude quotient used in many other studies (Alku *et al.*, 2002). The closed quotient (CQ; duration of the closed phase as a fraction of one oscillation cycle) was also extracted from the glottal flow waveform, as described in Zhang (2016). The measures of source acoustics include the fundamental frequency (F0), A-weighted source sound pressure level (SPL; calculated using the time derivative of the glottal flow waveform), cepstral peak prominence (CPP), the level differences between the first harmonic and the second harmonic (H1-H2), the fourth harmonic (H1-H4), the harmonic nearest 2 kHz (H1-H2k), and the harmonic nearest 5 kHz (H1-H5k) in the spectrum of the time derivative of the glottal flow waveform. The peak vocal fold contact pressure (Pc) over the medial surface was also calculated for each condition, as an indirect measure of risk of vocal fold injury.

A multi-factorial analysis of variance (ANOVA) was performed to quantify the main effects and two-way interaction effects of the model control parameters on different voice source measures. Higher-order interaction terms were not included because of missing data in some factorial combinations. The two depth controls (D_b and D_c), which were shown to have only small effects on the voice source (Zhang, 2021), were excluded from the ANOVAs to ensure that the dataset includes at least one condition that achieves sustained phonation for each two-way interaction. To further increase the power of the analysis, the 18 steps of the subglottal pressure were grouped into four levels: $P_s \leq 600$ Pa,

$600\,\mathrm{Pa} < P_s \leq 1200\,\mathrm{Pa}$, $1200\,\mathrm{Pa} < P_s \leq 1800\,\mathrm{Pa}$, $P_s > 1800\,\mathrm{Pa}$, and labeled as PSG0, PSG1, PSG2, and PSG3, respectively, and the four pressure groups were used in the analysis instead of the 18 pressure levels.

The effect sizes η^2 of each model control or interaction effect was calculated as the percentage of total variance that was accounted for by each control parameter or interaction term, as calculated from the ANOVA. Multiple comparisons with Bonferroni correction were made to further evaluate the general trends of variation of the voice source measures at different levels of individual control parameters or combination levels of control parameters.

Many interaction effects turned out to be small. Therefore, the following focuses on the interaction terms with relatively large effect sizes. It should be noted that, because of the large number of control parameters, the effect sizes were generally small, and the convention rules for determining whether an effect is moderate or large do not apply. In this study, for each voice source measure, the effect sizes were compared to the largest effect size of the specific source measure, and only terms with an effect size larger than 10% of the largest effect size were included for discussion below. However, all interaction terms were manually reviewed and were included in discussion if notable changes in trends (e.g., trend reversal) were observed across different levels, regardless of the effect size. Occasionally, some interaction effects with a smaller effect size were included in the discussion in order to highlight the lack of effect.

III. RESULTS

Figure 2 shows the overall trends of the effect sizes for different voice source measures. While different interaction terms became important for different measures, some trends can be observed. For example, relatively large effect sizes were observed for the interaction between the initial glottal angle and vertical thickness (denoted by $\alpha{*}T$ in Fig. 2) in the control of MFDRn, CQ, and the source spectral measures, as shown in Figs. 2(b) and 2(c). For the four spectral shape measures in Fig. 2(c), interactions were also observed between the vertical thickness and vocal fold stiffness in the longitudinal direction. For amplitude-based measures in Fig. 2(a), there were multiple interaction terms involving vocal fold length L, which disappeared when properly normalized (e.g., compare MFDR and MFDRn). For these amplitude-based measures, some relatively large interaction effects involving the subglottal pressure P_s can also be observed in Fig. 2(a), indicating effects that vary with vocal intensity. Figure 2(d) shows that the interaction effects were generally small for the control of F0 and SPL. In contrast, multiple moderate to large interaction effects can be observed for the control of the peak vocal fold contact pressure.

In the following, the major interaction effects are discussed for selected voice source measures. For completeness, the discussion for each source measure starts with the main effects, followed by interaction effects.

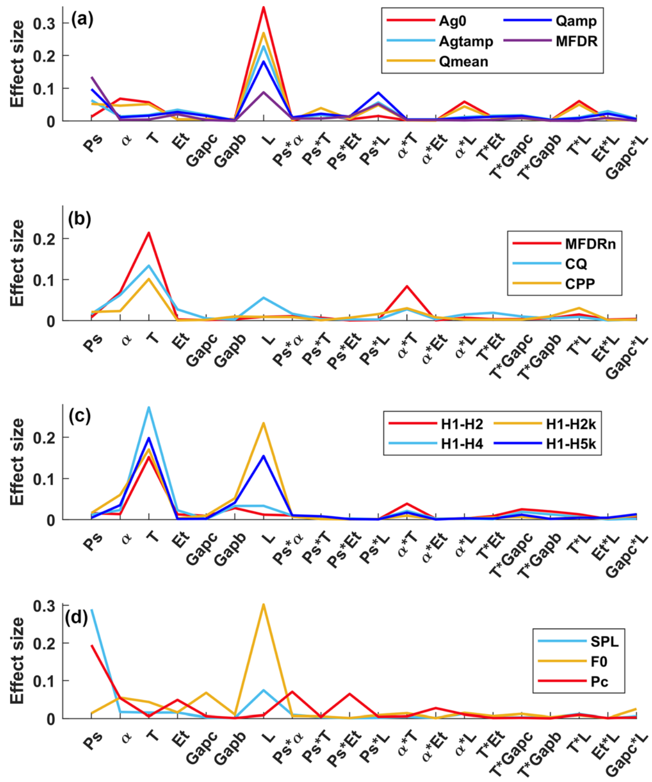

FIG. 2. (Color online) (a)–(d) Effect sizes of model control parameters and major interaction terms for selected voice source measures.

A. Mean glottal flow and MFDR

The following discusses the control of the mean glottal flow and MFDR. The main effects and interactions for the mean glottal area (Ag0) were similar to those for the mean glottal flow, whereas the control patterns for the peak-to-peak amplitudes of the glottal area (Agtamp) and glottal flow (Qamp) were similar to those for MFDR. For clarity, their controls are not discussed here.

The mean glottal flow increased with increasing vocal fold length, subglottal pressure, initial glottal angle, and decreased with increasing thickness, transverse stiffness, and AP stiffness in either the body or cover layer. Figure 3 shows the four largest interaction effects in the control of the mean glottal flow. Each panel shows the ANOVA-estimated averages of the mean glottal flow at different combination levels of selected control parameters. The first three interaction effects involved vocal fold length, with the effects of the subglottal pressure, thickness, and initial glottal angle becoming smaller in shorter vocal folds. These interactions reflect a length effect on the glottal flow, with longer vocal folds often consuming higher airflow and thus a larger flow range for other controls to apply influence.

There was also an interaction between subglottal pressure and vertical thickness [Fig. 3(d)], with the effect of subglottal pressure on the mean airflow decreasing with increasing thickness. For the thickest condition ($T = 4.5\,\mathrm{mm}$), the effect of subglottal pressure on the mean glottal flow was statistically insignificant. Thus, thicker folds are better able to maintain the adductory position and not be pushed open by

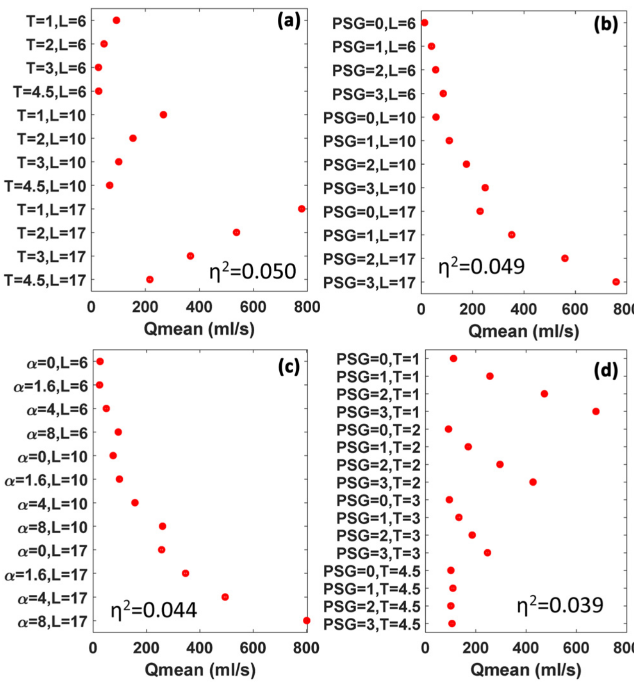

FIG. 3. (Color online) (a)–(d) Interaction effects on the mean glottal flow (Qmean). Each panel shows the ANOVA-estimated mean values of the mean glottal flow at different combination levels of selected control parameters (subglottal pressure group PSG, vertical thickness T, initial glottal angle α, and vocal fold length L).

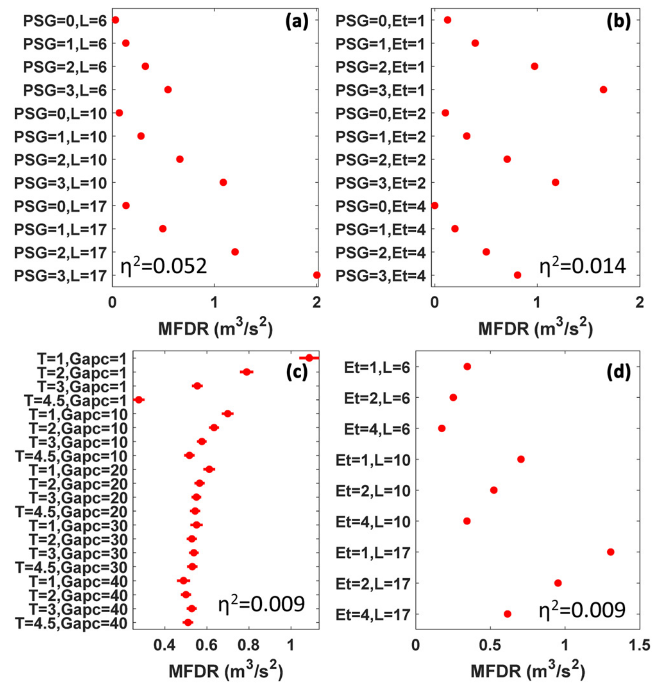

FIG. 4. (Color online) (a)–(d) Interaction effects on MFDR. Each panel shows the ANOVA-estimated mean values of MFDR at different combination levels of selected control parameters (subglottal pressure group PSG, vertical thickness T, vocal fold length L, transverse stiffness E_t, and AP cover stiffness G_{apc}).

subglottal pressure. It is worth noting that the effect of the three stiffness parameters (E_t, G_{apc}, G_{apb}) was small in general, and decreased with increasing vertical thickness.

MFDR increased with increasing subglottal pressure, increasing vocal fold length, and decreasing transverse stiffness of the vocal folds, with smaller main effects from the other controls. Interactions were observed involving the three controls with the largest main effects (i.e., pressure, length, and transverse stiffness; Fig. 4). The effect of subglottal pressure on MFDR reduced with decreasing vocal fold length [Fig. 4(a)] or increasing transverse stiffness [Fig. 4(b)]. Thus, the highest MFDR was reached in conditions with the largest vocal fold length, lowest transverse stiffness, and highest subglottal pressure. Figure 4(c) also shows that the effect of the vertical thickness was small in general but became large in conditions with low AP stiffness in the cover layer ($G_{apc} < 20$ kPa).

Note that in Fig. 4(c) there is a horizontal bar associated with each data point. The horizontal bars indicate comparison intervals, with the interval widths calculated in a way so that the difference in MFDR was statistically significant ($p < 0.005$ with Bonferroni correction) when two conditions have non-overlapping bars (Hochberg and Tamhane, 1987). Similar horizontal bars are present in Fig. 3, although they are too short to be seen.

B. CQ and MFDRn

Figure 2(b) shows that the CQ was dominantly controlled by the vertical thickness of the vocal fold medial surface, with the CQ increasing with increasing thickness, similar to findings in previous studies (Zhang, 2016, 2021). Figure 2(b) also shows a secondary effect of the other controls, with the CQ increasing with decreasing glottal gap, decreasing vocal fold length, and decreasing transverse stiffness.

Figure 5(a) shows that, while the initial glottal angle had a notable main effect size, this effect was mainly due to the relatively large values in CQ at the conditions with $\alpha = 0°$, particularly in thicker vocal folds. When this condition ($\alpha = 0°$) was excluded, changes in the initial glottal angle (from 1.6° to 8°) had only small effect on CQ. In general, the effect of the initial glottal gap increased with increasing thickness [Fig. 5(a)] or decreasing vocal fold length [Fig. 5(d)]. An interaction between the subglottal pressure and the initial glottal angle can be observed in Fig. 5(c), with increasing subglottal pressure increasing the CQ at non-zero initial glottal angles but decreasing CQ slightly for conditions with $\alpha = 0°$. This interaction effect can also be interpreted as a large effect of the initial glottal angle at low subglottal pressures (PSG0) or near phonation onset, where vocal fold approximation from a large-gap resting position significantly increased the CQ, as observed in our previous studies (Zhang, 2016). Figure 5(b) also shows that the effect of the thickness increased with decreasing transverse stiffness.

The normalized MFDRn was dominantly controlled by vocal fold vertical thickness, with MFDRn increasing with thickness. A secondary effect of the initial glottal gap was observed in Fig. 2(b). However, this effect was again due to the relatively large MFDRn values at conditions of $\alpha = 0°$ in thick vocal folds ($T = 3$ and 4.5 mm), as shown in Fig. 6(a).

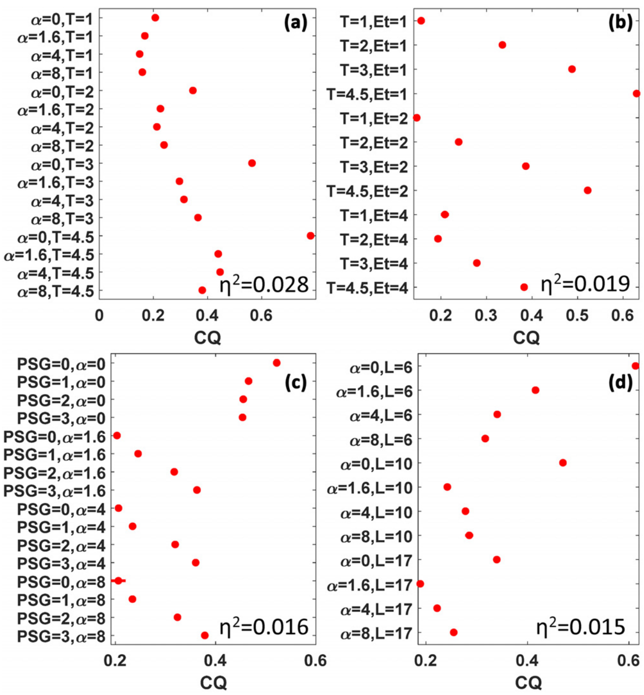

FIG. 5. (Color online) (a)–(d) Interaction effects on the CQ. Each panel shows the ANOVA-estimated mean values of CQ at different combination levels of selected control parameters (subglottal pressure group PSG, vertical thickness T, initial glottal angle α, vocal fold length L, and transverse stiffness E_t).

The effect of the subglottal pressure was small except for conditions with $\alpha = 0°$ [Fig. 6(c)] or in thick folds [$T > 2$ mm; Fig. 6(d)], at which increasing subglottal pressure decreased the MFDRn. This suggests that increasing pressure reduces skewing of the glottal flow waveform at conditions of tight vocal fold adduction. Thus, the highest MFDRn was reached in thick vocal folds fully medialized at low subglottal pressures, which often produced a pressed voice quality or even vocal fry (Zhang, 2018). Figure 6(b) also shows a small interaction effect between thickness and length.

C. Source spectral measures

Similar to CQ and MFDRn, the source spectral measures were dominantly controlled by vocal fold vertical thickness, as shown in Fig. 2(c). For H1-H2k and H1-H5k, there was also a large effect of vocal fold length. This effect was largely due to the large effect of vocal fold length on the fundamental frequency, which changes the frequency spacing between the first harmonic and the harmonic nearest 2 kHz and 5 kHz, the amplitude differences of which are measured by these two measures.

In general, H1-H2 decreased with increasing vertical thickness. Interaction between the initial glottal angle and vertical thickness was observed in the control of H1-H2. Figure 7(a) shows that H1-H2 decreased with increasing initial glottal angle in thin vocal folds ($T = 1$ mm). This trend was gradually reversed so that, for thick vocal folds, H1-H2 increased with increasing initial glottal angle [Fig. 7(a)]. Figure 7 also shows that the effect of vertical thickness on H1-H2 was larger for conditions of high AP stiffness in the cover layer [Fig. 7(b)] and low AP stiffness in the body layer [Fig. 7(c)]. An interaction between the subglottal pressure and initial glottal angle near phonation onset can also be observed in Fig. 7(d), which shows an increased effect of

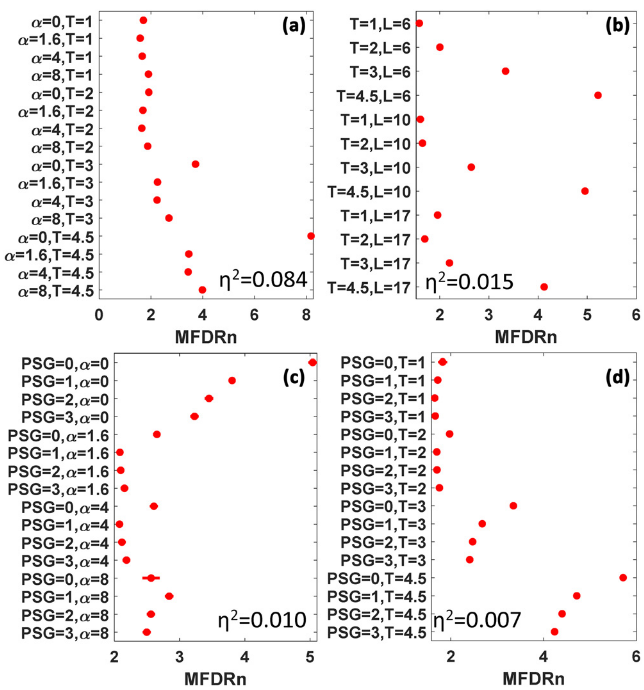

FIG. 6. (Color online) (a)–(d) Interaction effects on MFDRn. Each panel shows the ANOVA-estimated mean values of MFDRn at different combination levels of selected control parameters (subglottal pressure group PSG, vertical thickness T, initial glottal angle α, and vocal fold length L).

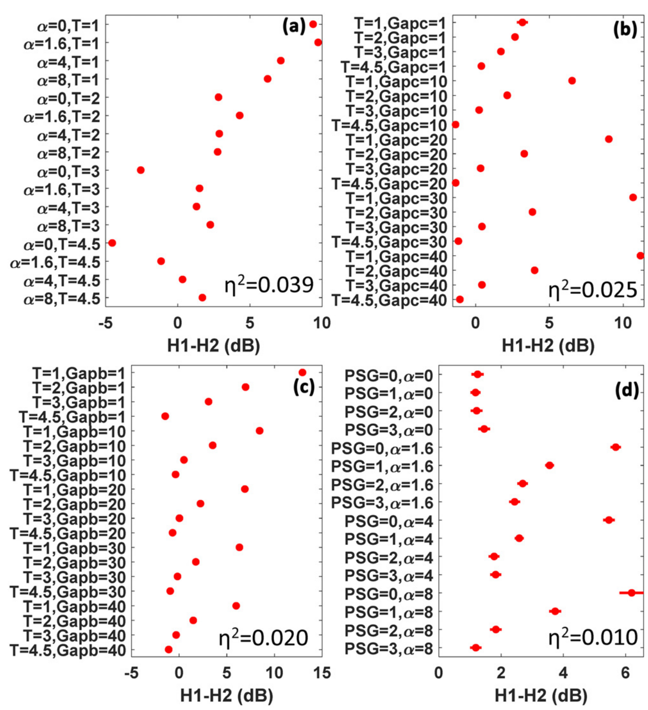

FIG. 7. (Color online) (a)–(d) Interaction effects on H1-H2. Each panel shows the ANOVA-estimated mean values of H1-H2 at different combination levels of selected control parameters (subglottal pressure group PSG, vertical thickness T, initial glottal angle α, AP cover stiffness G_{apc}, and AP body stiffness G_{apb}).

the subglottal pressure at non-zero initial glottal angles and a larger effect of the initial glottal angle at lower subglottal pressures (PSG0). This is presumably due to an improved glottal closure near phonation onset with either an increase in pressure or a decrease in the initial glottal angle, as shown earlier in Fig. 5(c) for the control of CQ.

Both H1-H2k and H1-H5k were dominantly controlled by the vertical thickness, with both decreasing with increasing thickness, indicating that thicker folds produce stronger mid- and high-frequency harmonics. H1-H2k also decreased with decreasing initial glottal angle [Fig. 8(b)], increasing AP stiffness in the cover layer [Figs. 8(a) and 8(d)]. Increasing subglottal pressure also decreased H1-H2k, although this effect was much reduced for conditions of $\alpha = 0°$. Similar trends can be observed for the control of H1-H5k (Fig. 9), although the interaction patterns, particularly between the subglottal pressure and initial glottal angle, were more complicated.

The CPP was mainly controlled by the vertical thickness [Fig. 2(b)], and increased with increasing thickness, particularly for long vocal folds [Fig. 10(b)], large initial glottal angles [Fig. 10(a)], and low AP stiffness in the body layer [Fig. 10(d)]. CPP also increased with decreasing initial glottal angle, particularly in thin vocal folds [Fig. 10(a)]. Increasing subglottal pressure generally decreased CPP [Fig. 10(c)], except for the shortest vocal folds for which CPP increased then decreased with increasing subglottal pressure.

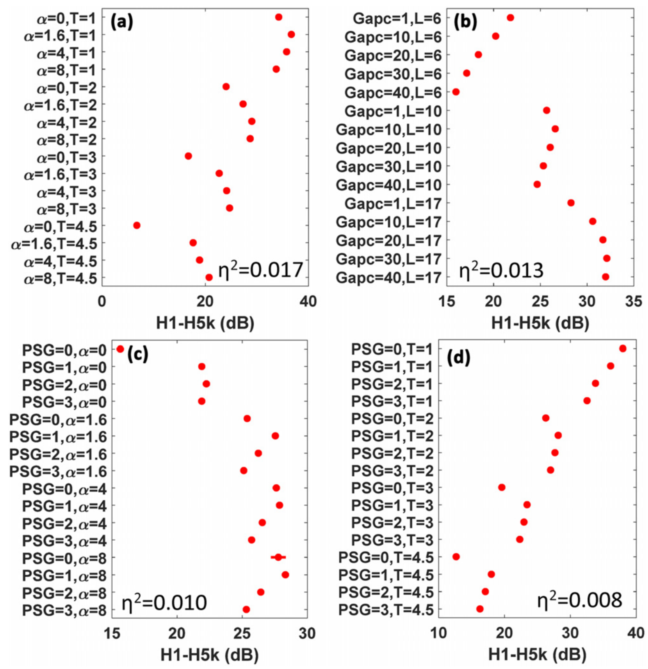

FIG. 9. (Color online) (a)–(d) Interaction effects on H1-H5k. Each panel shows the ANOVA-estimated mean values of H1-H5k at different combination levels of selected control parameters (subglottal pressure group PSG, vertical thickness T, initial glottal angle α, vocal fold length L, and AP cover stiffness G_{apc}).

D. F0 and SPL

For the fundamental frequency F0, vocal fold length had the largest effect size, with the F0 increasing with decreasing vocal fold length. F0 can be increased, in the order of decreasing effect size, by decreasing vocal fold length, increasing AP stiffness in the cover layer G_{apc}, decreasing initial glottal angle α, decreasing vertical thickness T, increasing transverse stiffness E_t, increasing

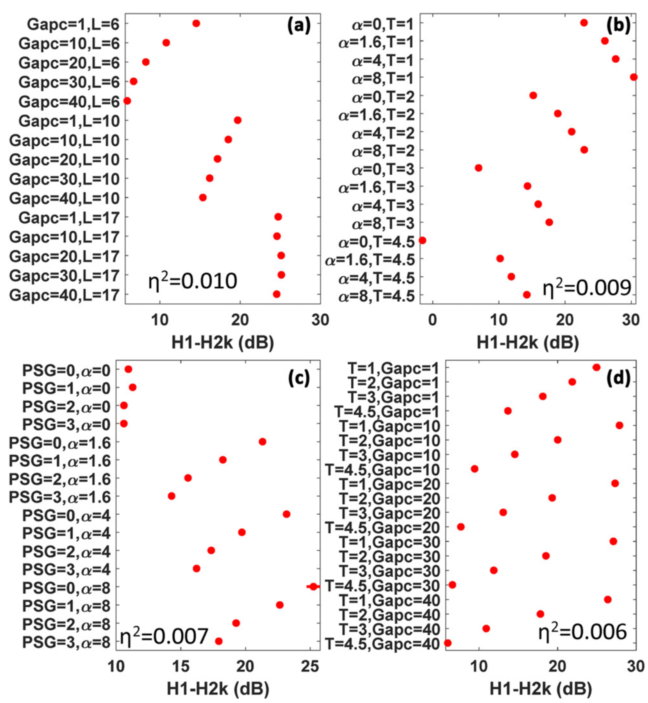

FIG. 8. (Color online) (a)–(d) Interaction effects on H1-H2k. Each panel shows the ANOVA-estimated mean values of H1-H2k at different combination levels of selected control parameters (subglottal pressure group PSG, vertical thickness T, initial glottal angle α, vocal fold length L, and AP cover stiffness G_{apc}).

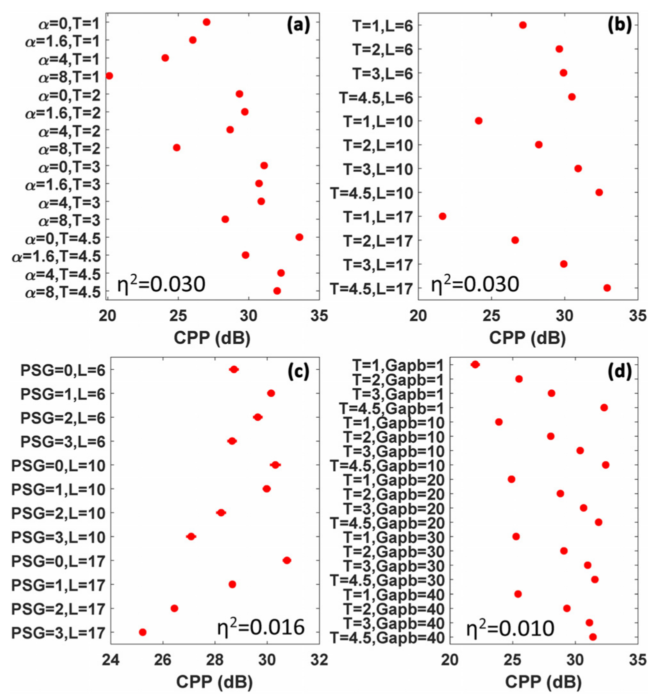

FIG. 10. (Color online) (a)–(d) Interaction effects on CPP. Each panel shows the ANOVA-estimated mean values of CPP at different combination levels of selected control parameters (subglottal pressure group PSG, vertical thickness T, initial glottal angle α, vocal fold length L, and AP body stiffness G_{apb}).

subglottal pressure P_s, and increasing AP stiffness in the body layer G_{apb}. Note that the AP stiffness in the body layer had a much smaller effect on F0 than the AP stiffness in the cover layer, indicating that cover layer properties had a larger impact on F0 than body-layer properties.

Figure 11(d) shows that the effect of the subglottal pressure on F0 was much reduced in thin vocal folds. This suggests that the F0-increasing effect of increasing pressure is likely associated with the increase in the duration of vocal fold contact, which is lower in thinner vocal folds. In contrast, the effect of initial glottal angle on F0 is likely associated with the increase in the spatial extent of vocal fold contact along the AP direction, which increases with decreasing initial glottal angle. Thus, the F0 decreased monotonically with increasing initial glottal angle in thin vocal folds [Fig. 11(b)], whereas in thick folds the F0 first increased with increasing initial glottal angle (likely associated with increased vibration amplitude) then decreased with further increase in the initial glottal angle, due to probably reduced extent of vocal fold contact along the AP direction.

Figure 11(c) also shows that the effect of AP stiffness in the cover layer was larger in thinner vocal folds, indicating a potential synergy between these two parameters in increasing F0 that may occur with the activation of the cricothyroid muscles. There were also interactions involving vocal fold length, with the effects of the AP cover stiffness, initial glottal angle, and subglottal pressure much larger in shorter vocal folds, an example of which is shown in Fig. 11(a). This is likely due to the higher F0 in shorter vocal folds and thus a larger range of F0 for other controls to influence.

Vocal intensity SPL was dominantly controlled by the subglottal pressure, with the SPL increasing with increasing subglottal pressure. There was also a relatively large effect of vocal fold length, with the SPL increasing with increasing length. The effect of the initial glottal angle on SPL was small, except in short [Fig. 12(a)] or thick vocal folds [Fig. 12(c)], or at low subglottal pressures (not shown). In general, the SPL was higher in thinner vocal folds [Fig. 12(b)], except for long vocal folds in which the maximum SPL was reached at an intermediate thickness. Figure 12(c) shows a trade-off between the initial glottal angle and vertical thickness in achieving a local maximum in SPL: while the SPL decreased with increasing thickness in general, a local maximum of SPL can be achieved in either thin vocal folds with a small initial glottal angle or thick vocal folds with a relatively large initial glottal angle. The existence of a range of optimal laryngeal configurations suggest that speakers may increase vocal efficiency using different laryngeal strategies, not necessarily limited to a barely abducted laryngeal configuration as often targeted in voice therapy.

E. Peak vocal fold contact pressure

The peak vocal fold contact pressure over the medial surface was dominantly controlled by subglottal pressure, whose effect size was much larger than all other control parameters [Fig. 2(d)], with the peak contact pressure increasing with increasing subglottal pressure. The transverse stiffness E_t had the third largest effect size, with the

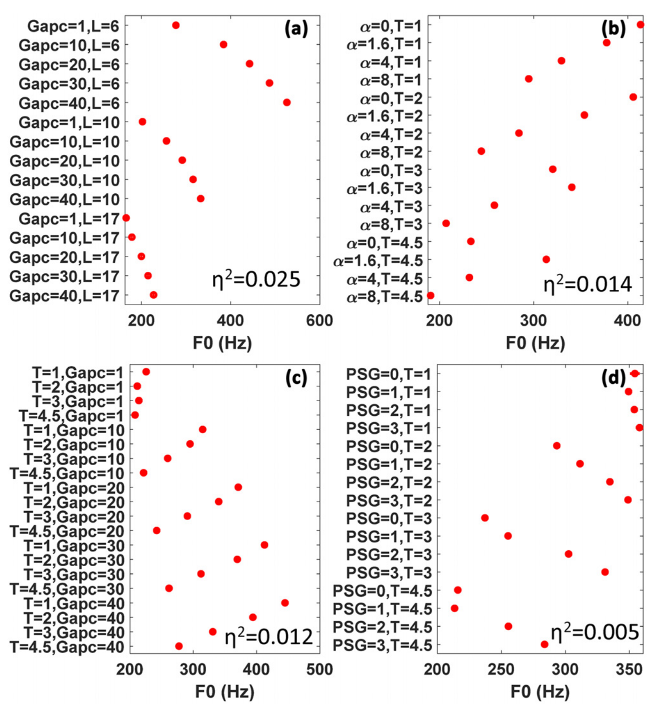

FIG. 11. (Color online) (a)–(d) Interaction effects on F0. Each panel shows the ANOVA-estimated mean values of F0 at different combination levels of selected control parameters (subglottal pressure group PSG, vertical thickness T, initial glottal angle α, vocal fold length L, and AP cover stiffness G_{apc}).

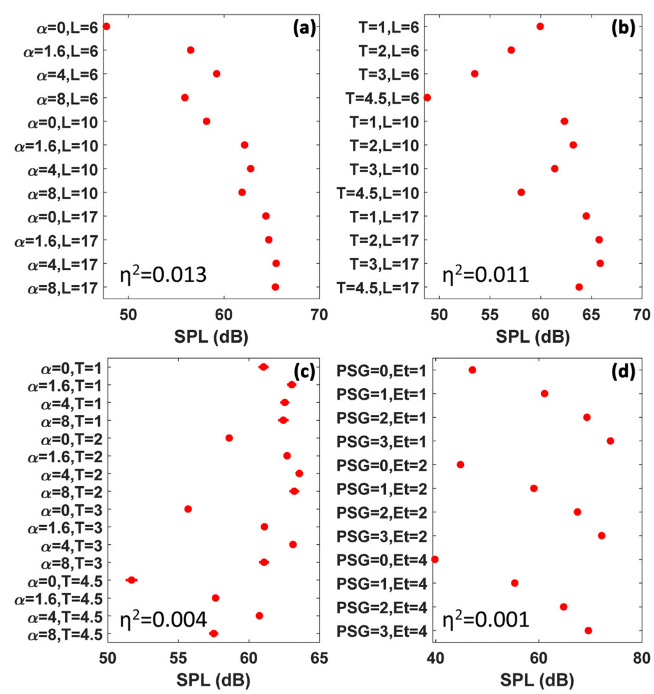

FIG. 12. (Color online) (a)–(d) Interaction effects on SPL. Each panel shows the ANOVA-estimated mean values of SPL at different combination levels of selected control parameters (subglottal pressure group PSG, vertical thickness T, initial glottal angle α, vocal fold length L, and transverse stiffness E_t).

JASA
https://doi.org/10.1121/10.0034708

peak contact pressure increasing with decreasing transverses stiffness. Figure 13(b) shows that the combination of low transverse stiffness and high subglottal pressure produced a peak contact pressure that was much higher than the simple addition of the two main effects. Therefore, when increasing vocal intensity, it is important to maintain a balance between subglottal pressure and transverse stiffness. To prevent excessively high vocal fold contact pressure, transverse stiffness should be increased together with the increase in subglottal pressure. It is worth noting that increasing transverse stiffness has only a minimal effect on SPL [Fig. 12(d)]. This makes it an effective strategy for reducing peak vocal fold contact pressure without significantly diminishing SPL.

The initial glottal angle had the second largest effect size. However, this large effect size was largely due to the extremely low contact pressure at the largest initial glottal angle [$\alpha = 8°$; Figs. 13(a), 13(c), 13(d), and 13(f)], as occurs for example in breathy phonation. If this largest gap condition was excluded, changes in the initial glottal angle between 0° and 4° had only small effect on vocal fold contact pressure, and this effect was smaller than the effect of the transverse stiffness [Fig. 13(c)], vocal fold length [Fig. 13(d)], or even the vertical thickness [Fig. 13(f)]. In general, the peak vocal fold contact pressure increased with increasing vocal fold thickness, decreasing vocal fold length, and increasing AP stiffness in the cover layer, although these effects were much smaller than the effects of the subglottal pressure and transverse stiffness. The effect of AP stiffness in the body layer on the peak vocal fold contact pressure was generally small.

IV. DISCUSSION

The goal of this study was to identify important two-way interaction effects and provide a more complete picture of laryngeal and respiratory control of voice production that might be missing from the main effects identified in our previous studies. While the importance of different interaction effects varied with the specific source measure, one important interaction effect was observed between the initial glottal angle (a measure of horizontal prephonatory glottal gap) and medial surface vertical thickness, particularly in the control of glottal closure and voice source spectral shape. While both the glottal closure pattern and voice source spectra were dominantly controlled by vocal fold vertical

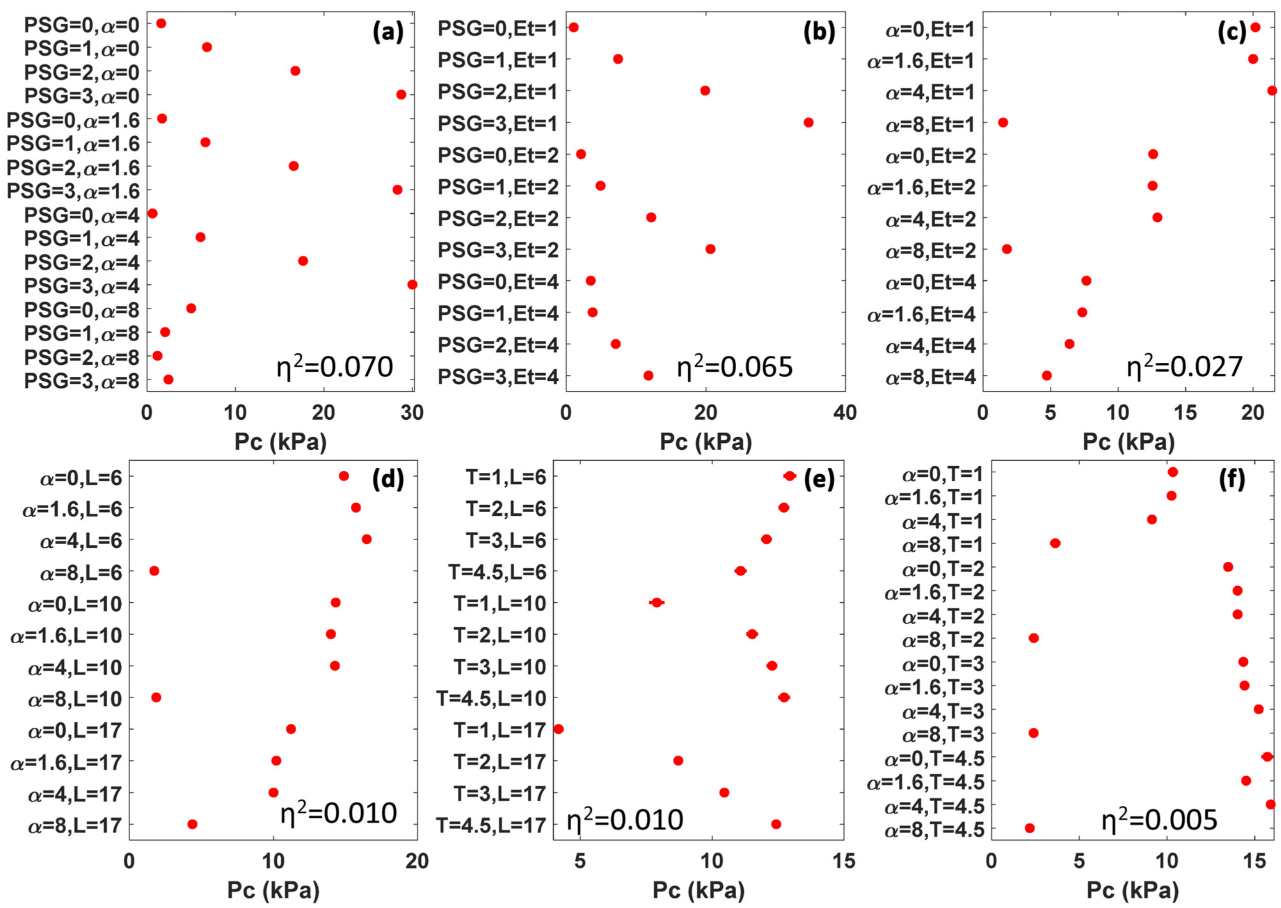

FIG. 13. (Color online) (a)–(f) Interaction effects on peak vocal fold contact pressure. Each panel shows the ANOVA-estimated mean values of Pc at different combination levels of selected control parameters (subglottal pressure group PSG, vertical thickness T, initial glottal angle α, vocal fold length L, and transverse stiffness E_t).

thickness, changes in the initial glottal angle can have large effects in thick vocal folds. In particular, complete vocal fold medialization (i.e., a zero initial glottal angle), together with vocal fold thickening, is required to produce the highest values in CQ and MFDRn and the least steep source spectral slope (i.e., lowest H1-H2, H1-H2k, and H1-H5k), as for example in the production of a pressed voice. However, this strong high-frequency harmonic production comes at the costs of reduced vocal efficiency [Fig. 12(c)] and increased vocal fold contact pressure [Fig. 13(f)], which may not be desirable. A more efficient and healthy way to increase high-frequency harmonic production is to adopt a less tight laryngeal configuration (see discussion below) and rely on vocal tract resonance to amplify mid- and high-frequency harmonics (e.g., singer's formant clustering or formant tuning).

Our results also provide a more complete picture of laryngeal and respiratory strategies to reduce the peak vocal fold contact pressure and risk of vocal fold injury. The peak vocal fold contact pressure is dominantly controlled by subglottal pressure and, to a lesser extent, transverse stiffness. There is a significant interaction effect between these two parameters so that low transverse stiffness combined with high subglottal pressure produces a contact pressure that is much higher than the simple addition of the two main effects. Considering the dominantly large effect size of subglottal pressure on the peak vocal fold contact pressure, the most effective way to reduce contact pressure is to reduce subglottal pressure. Unfortunately, reducing subglottal pressure alone also significantly diminishes vocal intensity. Thus, to minimize vocal fold contact pressure and risk of vocal fold injury when producing a loud voice, it is important to balance an increase in subglottal pressure with a simultaneous increase in transverse stiffness. This is particularly important when producing high-intensity voices, where increasing transverse stiffness has small impact on vocal intensity [Fig. 12(d)] but significantly reduces the peak vocal fold contact pressure [Fig. 13(b)], as previously shown in Zhang (2020). In humans, increasing vocal intensity is often accompanied by an increase in fundamental frequency. It is thus important that this increase in fundamental frequency when increasing intensity is achieved through actions of the cricothyroid muscles, which elongate the vocal folds and increase transverse stiffness (Zhang *et al.*, 2017), rather than predominantly using the thyroarytenoid muscles, which reduces transverse stiffness in the cover layer.

An alternative way to reduce contact pressure while still being heard is to lower the subglottal pressure required to produce a target radiated SPL, through laryngeal and/or vocal tract adjustments. Previous studies (Titze and Talkin, 1979; Gauffin and Sundberg, 1989; Verdolini *et al.*, 1998; Berry *et al.*, 2001; Titze, 2006) have shown that maximum vocal efficiency can be achieved at an intermediate initial glottal gap (e.g., an inter-vocal process distance of about 0.6 mm) (Berry *et al.*, 2001), which is often targeted in voice therapy to improve vocal efficiency and minimize vocal injury. Similar findings were observed in our study. However, our study showed not one, but a continuum of such optimal adduction configurations characterized by a trade-off between the initial glottal gap and thickness: from thin folds tightly approximated (i.e., a small initial glottal angle) to thick folds loosely approximated. This finding implies that voice therapy could be more effective by focusing on a wide range of optimal laryngeal configurations, balancing the prephonatory gap and vertical thickness, instead of solely targeting the initial glottal gap.

This study also showed important interaction effects near phonation onset between the subglottal pressure and the initial glottal angle. For example, for non-zero initial glottal angles ($\alpha > 0°$), increasing subglottal pressure increased the CQ and high-frequency harmonic production (i.e., decreased H1-H2k and H1-H5k). However, this effect was much smaller at conditions with $\alpha = 0°$. This may be related to that fact that, at large initial glottal angles, high subglottal pressures are required to produce a sufficiently large vibration amplitude and initiate contact between the two vocal folds. A similar interaction can be observed for the peak vocal fold contact pressure, which increases with increasing subglottal pressure for small initial glottal angles but not for the largest initial glottal angle ($\alpha = 8°$).

Many interaction effects involving vocal fold length were observed in this study. Some of these interactions are simply a scaling effect of length, particularly for amplitude-based measures and F0. For example, the effect of the initial glottal angle on the mean glottal flow was larger in longer vocal folds. However, other interaction effects are for normalized measures and thus indicate potentially size-related difference in voice production. For example, while the effect of the AP stiffness in the cover layer on H1-H2k and H1-H5k was small in long vocal folds, this effect was much larger in short vocal folds ($L = 6$ mm; corresponding to 8–10 years old) (Titze, 1989), with increasing AP cover stiffness decreasing both measures (i.e., stronger harmonic production at high frequencies). Vocal fold adduction (both the initial glottal angle and thickness) also had a more important effect on SPL in shorter vocal folds. These results point to potential differences in vocal control between children and adults, which is worth further investigation.

A limitation of this study is that no vocal tract was included in the simulations. While source-filter interaction is expected to be small in speech conditions where the fundamental frequency is well below the first resonance of the sub- or supra-glottal tract, the presence of a vocal tract can significantly impact the vocal fold contact pressure (see, e.g., Zhang, 2019). Also, because no vocal tract was included in this study, the SPL was calculated using the time derivative of the glottal flow and was almost entirely determined by the amplitude of the first harmonic (or second harmonic in the case of a pressed voice). This is different from the radiated SPL when a vocal tract is present, which is mostly determined by the harmonic closest to the first formant. The impact of source-filter interaction on the interaction effects will be addressed in future studies.

V. CONCLUSION

Laryngeal and respiratory control of the voice source was dominated by main effects. However, some important interaction effects were observed. While the glottal closure pattern and voice source spectra were primarily controlled by vocal fold vertical thickness, interaction between the prephonatory glottal gap and medial surface thickness was observed, and a coordinated increase in vocal fold approximation and vocal fold thickening is required to produce voices with a long duration of the closed phase and strong high-frequency harmonic production. Interaction between subglottal pressure and transverse stiffness of the vocal folds indicates the importance of balancing an increase in subglottal pressure with simultaneous increase in transverse stiffness to minimizing vocal fold injury, particularly in high-intensity voice production. Interactions near phonation onset were also observed.

ACKNOWLEDGMENTS

This work was supported by National Institute on Deafness and Other Communication Disorders, National Institutes of Health Research Grant No. R01 DC020240.

AUTHOR DECLARATIONS

Conflict of Interest

The author has no conflicts to disclose.

DATA AVAILABILITY

The data that support the findings of this study are available from the author upon reasonable request.

Alipour-Haghighi, F., and Titze, I. R. (**1991**). "Elastic models of vocal fold tissues," J. Acoust. Soc. Am. **90**(3), 1326–1331.
Alku, P., Bäckström, T., and Vilkman, E. (**2002**). "Normalized amplitude quotient for parametrization of the glottal flow," J. Acoust. Soc. Am. **112**(2), 701–710.
Alzamendi, G. A., Peterson, S. D., Erath, B. D., Hillman, R. E., and Zañartu, M. (**2022**). "Triangular body-cover model of the vocal folds with coordinated activation of the five intrinsic laryngeal muscles," J. Acoust. Soc. Am. **151**(1), 17–30.
Berry, D., Verdolini, K., Montequin, D. W., Hess, M. M., Chan, R. W., and Titze, I. R. (**2001**). "A quantitative output-cost ratio in voice production," J. Speech Lang. Hear. Res. **44**, 29–37.
Döllinger, M., Zhang, Z., Schoder, S., Šidlof, P., Tur, B., and Kniesburges, S. (**2023**). "Overview on state-of-the-art numerical modeling of the phonation process," Acta Acust. **7**, 25.
Gauffin, J., and Sundberg, J. (**1989**). "Spectral correlates of glottal voice source waveform characteristics," J. Speech Lang. Hear. Res. **32**, 556–650.
Hirano, M., and Kakita, Y. (**1985**). "Cover-body theory of vocal fold vibration," in *Speech Science: Recent Advances*, edited by R. G. Daniloff (College-Hill, San Diego), pp. 1–46.
Hochberg, Y., and Tamhane, A. C. (**1987**). *Multiple Comparison Procedures* (Wiley, New York), Chap. 3, pp. 96–98.
Hollien, H. (**1960**). "Vocal pitch variation related to changes in vocal fold length," J. Speech Hear. Res. **3**(2), 150–156.
Hollien, H., and Curtis, F. (**1960**). "A laminagraphic study of vocal pitch," J. Speech Hear. Res. **3**(4), 361–371.
Holmberg, E., Hillman, R., and Perkell, J. (**1988**). "Glottal airflow and transglottal air pressure measurements for male and female speakers in soft, normal, and loud voice," J. Acoust. Soc. Am. **84**(2), 511–529.
Li, S., Scherer, R. C., Fulcher, L. P., Wang, X., Qiu, L., Wan, M., and Wang, S. (**2018**). "Effects of vertical glottal duct length on intraglottal pressures and phonation threshold pressure in the uniform glottis," J. Voice **32**(1), 8–22.
Li, Z., Chen, Y., Chang, S., and Luo, H. (**2020**). "A reduced-order flow model for fluid–structure interaction simulation of vocal fold vibration," J. Biomech. Eng. **142**(2), 021005.
Luizard, P., Bailly, L., Yousefi-Mashouf, H., Girault, R., Orgéas, L., and Henrich Bernardoni, N. (**2023**). "Flow-induced oscillations of vocal-fold replicas with tuned extensibility and material properties," Sci. Rep. **13**(1), 22658.
Madill, C., and Nguyen, D. D. (**2023**). "Impact of instructed laryngeal manipulation on acoustic measures of voice–preliminary results," J. Voice **37**(1), 143.e1–143.e11.
McCollum, I., Throop, A., Badr, D., and Zakerzadeh, R. (**2023**). "Gender in human phonation: Fluid–structure interaction and vocal fold morphology," Phys. Fluids **35**(4), 041907.
Pickup, B. A., and Thomson, S. L. (**2011**). "Identification of geometric parameters influencing the flow-induced vibration of a two-layer self-oscillating computational vocal fold model," J. Acoust. Soc. Am. **129**(4), 2121–2132.
Scherer, R. C., Shinwari, D., De Witt, K. J., Zhang, C., Kucinschi, B. R., and Afjeh, A. A. (**2001**). "Intraglottal pressure profiles for a symmetric and oblique glottis with a divergence angle of 10 degrees," J. Acoust. Soc. Am. **109**(4), 1616–1630.
Sundberg, J. (**2017**). "An effect of source-filter interaction on amplitudes of source spectrum partials," in *Proceedings of the 10th International Workshop on Models and Analysis of Vocal Emissions for Biomedical Applications, MAVEBA 2017*, December 13–15, Firenze, Italy, pp. 95–98.
Titze, I. (**2006**). "Voice training and therapy with a semi-occluded vocal tract: Rationale and scientific underpinnings," J. Speech Lang. Hear. Res. **49**, 448–459.
Titze, I. R. (**1989**). "Physiologic and acoustic differences between male and female voices," J. Acoust. Soc. Am. **85**(4), 1699–1707.
Titze, I. R. (**2008**). "Nonlinear source–filter coupling in phonation: Theory," J. Acoust. Soc. Am. **123**(4), 1902–1915.
Titze, I., and Talkin, D. (**1979**). "A theoretical study of the effects of various laryngeal configurations on the acoustics of phonation," J. Acoust. Soc. Am. **66**(1), 60–74.
Tur, B., Gühring, L., Wendler, O., Schlicht, S., Drummer, D., and Kniesburges, S. (**2023**). "Effect of ligament fibers on dynamics of synthetic, self-oscillating vocal folds in a biomimetic larynx model," Bioengineering **10**(10), 1130.
Verdolini, K., Druker, D., Palmer, P., and Samawi, H. (**1998**). "Laryngeal adduction in resonant voice," J. Voice **12**, 315–327.
Wang, X., Jiang, W., Zheng, X., and Xue, Q. (**2021**). "A computational study of the effects of vocal fold stiffness parameters on voice production," J. Voice **35**(2), 327.e1–327.e11.
Wu, L., and Zhang, Z. (**2016**). "A parametric vocal fold model based on magnetic resonance imaging," J. Acoust. Soc. Am. **140**(2), EL159–EL165.
Zhang, Z. (**2016**). "Cause-effect relationship between vocal fold physiology and voice production in a three-dimensional phonation model," J. Acoust. Soc. Am. **139**(4), 1493–1507.
Zhang, Z. (**2017**). "Effect of vocal fold stiffness on voice production in a three-dimensional body-cover phonation model," J. Acoust. Soc. Am. **142**(4), 2311–2321.
Zhang, Z. (**2018**). "Vocal instabilities in a three-dimensional body-cover phonation model," J. Acoust. Soc. Am. **144**(3), 1216–1230.
Zhang, Z. (**2019**). "Vocal fold contact pressure in a three-dimensional body-cover phonation model," J. Acoust. Soc. Am. **146**(1), 256–265.
Zhang, Z. (**2020**). "Laryngeal strategies to minimize vocal fold contact pressure and their effect on voice production," J. Acoust. Soc. Am. **148**, 1039–1050.
Zhang, Z. (**2021**). "Contribution of laryngeal size to differences between male and female voice production," J. Acoust. Soc. Am. **150**(6), 4511–4521.
Zhang, Z. (**2023a**). "The influence of source-filter interaction on the voice source in a three-dimensional computational model of voice production," J. Acoust. Soc. Am. **154**(4), 2462–2475.
Zhang, Z. (**2023b**). "Vocal fold vertical thickness in human voice production and control: A review," J. Voice (in press).
Zhang, Z., Samajder, H., and Long, J. (**2017**). "Biaxial mechanical properties of human vocal fold cover under vocal fold elongation," J. Acoust. Soc. Am. **142**(4), EL356–EL361.